pH Dependence of Bacteriorhodopsin Thermal Unfolding†

Christie G. Brouillette,*,‡ Donald D. Muccio,§ and Teresa K. Finney‡

Departments of Medicine and Chemistry, University of Alabama at Birmingham, Birmingham, Alabama 35294

Received March 16, 1987; Revised Manuscript Received June 18, 1987

ABSTRACT: The thermal denaturation of bacteriorhodopsin in the purple membrane of *Halobacterium halobium* has been studied by differential scanning calorimetry (DSC) and temperature-dependent spectroscopy in the pH range from 5 to 11. Monitoring of protein fluorescence and absorbance in the near-UV and visible regions indicates that changes primarily occur in tertiary structure with denaturation. Far-UV circular dichroism shows only small changes in the secondary structure, unlike most globular water-soluble proteins of comparable molecular weight. The DSC transition can best be described as a two-state denaturation of the trimer. Thermodynamic analysis of the calorimetric transition reveals some similarity between the unfolding of bacteriorhodopsin and water-soluble proteins. Specifically, a pH dependence of the midpoint temperature of denaturation is seen as well as a temperature-dependent enthalpy of denaturation. Proteolysis experiments on denatured purple membrane suggest that bacteriorhodopsin may be partially extruded from the membrane as it denatures. Exposure of buried hydrophobic residues to the aqueous environment upon denaturation is consistent with the observed temperature-dependent enthalpy.

The purple membrane of *Halobacterium* may be the best available completely native membrane system on which to attempt a thermodynamic analysis (Marque et al., 1984; Tristram-Nagle et al., 1986). This membrane exists in a functionally specialized and discretely localized region of the bacterium cell membrane and is composed of approximately 75% protein and 25% lipid (Henderson, 1977). The only protein component, bacteriorhodopsin, is a single polypeptide chain of 248 residues, which are threaded back and forth through the membrane (Oesterhelt & Stoeckenius, 1971; Khorana et al., 1979; Ovchinnikov et al., 1979). As a consequence of this arrangement, about 80% of the protein resides within the membrane. The extramembranous sequences that link these excursions across the membrane are predicted to be short. No more than 10 residues per loop (Engelman et al., 1980; Agard & Stroud, 1982) and only about 21 residues of the carboxyl terminus (Wallace & Henderson, 1982) and 8 or less residues of the amino terminus are outside the membrane. In 1975, Henderson and Unwin reported this chain topology to appear as seven roughly parallel rods in a low-resolution electron diffraction image. The secondary structure of these rods is still an open question, however (Lewis et al., 1985), and estimates of their α-helicity range from 60 to nearly 100% (Becher & Cassim, 1976; Mao & Wallace, 1984; Nabedryk et al., 1985), while β-structure and random coil have recently been suggested to contribute the remainder (Jap et al., 1983; Downer et al., 1986; Earnest & Rothschild, 1986). The low-resolution picture of bacteriorhodopsin was made possible by the unique organization of this protein in the native membrane, where it exists as a two-dimensional crystalline array of hexagonally packed trimers. The functional significance of this macroscopic organization of trimers is unclear, since bacteriorhodopsin also functions as a light-driven proton pump in the monomeric state (Dencher et al., 1983).

We report here a structural and thermodynamic description of the thermal denaturation of bacteriorhodopsin in the purple membrane. This investigation was undertaken in order to gain a more detailed picture of membrane protein stability and represents the first report in which the denaturation of a membrane protein has been studied by systematically changing a single solution variable, namely, pH. These studies have given us a closer look at the mechanism of membrane protein unfolding and reveal both similarities and differences in unfolding between this class and soluble proteins. A preliminary report of this work has appeared (Brouillette et al., 1986).

Materials and Methods

Purple Membrane Preparation. Halobacterium halobium S9 was grown in a laboratory-built fermentor equipped with fluorescent lights. The purple membrane was isolated and purified according to the procedure of Becher and Cassim (1975), usually with the elimination of the sucrose gradient as the final step. Protein concentrations were determined spectrophotometrically with an extinction coefficient at 568 nm of 63 mM^{-1} cm^{-1} (Oesterhelt & Stoeckenius, 1971).

Proteolysis and Gel Electrophoresis of Purple Membrane. To a solution containing 22 μg of purple membrane (2 mg/mL protein in 50 mM Tris,[1] pH 6.8) was added 17 μL of a papain (Worthington) stock solution (0.6 mg/mL in 1 mM EDTA, 6.7 μM mercaptoethanol, 5 mM cysteine) plus 33 μL of 3 M NaCl. The reaction mixture was then shaken in a 37 °C warm room for 20 h, after which time 10 mL of a solution of 1 M NaCl and 10 mM Tris, pH 6.8, was added. The proteolyzed membrane was centrifuged and washed, followed by a second centrifugation with 10 mM Tris, pH 8, which removed all

†This work was supported, in part, by NIH Grant GM-35474 (C.G.B.). T.K.F. was the recipient of a 1984 UAB Medical Student Summer Research Fellowship and received the first place award for her work on this project. On Oct 24, 1986, she died in a car accident and subsequently was awarded her M.D. degree posthumously on May 17, 1987. She received the outstanding student award in obstetrics and gynecology, which in future years will be presented in her honor. This paper is dedicated to her memory.

* Author to whom correspondence should be addressed.

‡ Department of Medicine.

§ Department of Chemistry.

[1] Abbreviations: CD, circular dichroism; DSC, differential scanning calorimetry; EDTA, ethylenediaminetetraacetic acid; ΔH_{cal}, calorimetric enthalpy; ΔH_{vH}, van't Hoff enthalpy; λ_{max}, absorbance maximum; NMR, nuclear magnetic resonance; PAGE, polyacrylamide gel electrophoresis; SDS, sodium dodecyl sulfate; Tris, tris(hydroxymethyl)aminomethane; T_m, midpoint temperature.

0006-2960/87/0426-7431$01.50/0

traces of papain as judged by SDS–PAGE. All membrane samples were prepared for electrophoresis by suspension in the pH 8 Tris buffer, followed by the addition of an equivalent volume of 0.125 M Tris, 4% SDS, and 20% glycerol, pH 6.8. These samples were then electrophoresed on a SDS–12–20% linear gradient polyacrylamide gel with a 4% stacker.

Calorimetry. Experiments were performed with either a Microcal MC-1 differential scanning calorimeter (Amherst, MA), which contains matched 1-mL platinum cells, or a Microcal MC-2, which contains matched tantalum cells. Equivalent volumes of sample and reference buffer were delivered into their respective cells after deaeration at 20 mmHg for 10–20 min. Purple membrane was suspended in 50 mM buffer containing 100 mM NaCl at the indicated pH. Where phosphate buffer was used, the buffer concentration was 190 mM without NaCl and was adjusted with either HCl or NaOH for pH values below 6 and above 9, respectively. The pH of each purple membrane suspension was checked before and after calorimetry, and none changed by more than 0.2 pH unit after heating. Some of the buffers used exhibit a significant temperature-dependent apparent pK_a. In some cases, therefore, the pH expected at the midpoint temperature (T_m) of bacteriorhodopsin denaturation is reported, as well as the pH measured at 25 °C, by measurement of the pH at T_m with a bacteriorhodopsin sample and/or by calculation with literature values for the temperature coefficient of the pK_a (Good et al., 1966). Unless otherwise indicated, the pH reported was measured at 25 °C. DSC scans were run on bacteriorhodopsin at concentrations from 90 to 130 μM, and scan rates were varied from 15 to 90 °C/h. The calorimeter was interfaced with an IBM XT for automatic data collection using a Data Translation DT-2805 A/D converter board (Marlboro, MA). Data collection and analysis programs were part of the CALSOFT package obtained from EMF Software (Knoxville, TN), which marketed this software exclusively for use with the MC-1 calorimeter. Data analysis software, available from Microcal for operation with the MC-2, was also used for calculating calorimetric and van't Hoff enthalpies. The DSC base lines are not completely flat, even when the reference and sample cells are perfectly matched with the same solution. We found the most reliable base line to substract from the initial heat capacity profile was that obtained from repeated scans of the denatured sample under study, since the denaturation transition is essentially irreversible. The T_m for a given transition was taken to be the point of maximum excess heat capacity, and the enthalpy was estimated from the total area under the curve.

Visible Absorption Spectroscopy. Spectra were recorded on a Gilford Reponse spectrophotometer in a 1-cm cell. The suspension of purple membrane, 9–10 μM bacteriorhodopsin in the appropriate buffer (50 mM) and 100 mM NaCl, was flushed with N_2, followed by equilibration at each temperature in the spectrophotometer prior to measurement. The spectrophotometer was equipped with a thermoelectric cell holder for heating and monitoring the temperature of the cuvette.

Fluorescence Spectroscopy. Emission spectra are uncorrected and were recorded on an American Scientific SPF scanning spectrofluorometer with a 300-nm cutoff filter and polarization filter placed in front of the emission light and an orthogonally placed polarization filter in front of the excitation beam. Excitation was at 289 nm; emission and excitation band-passes were 15 nm. Reported spectra were obtained on dark-adapted bacteriorhodopsin, 7 μM in 50 mM glycine and 100 mM NaCl, pH 8. The temperature of the sample compartment was raised at a constant rate of about 60 deg/h with a Lauda K2/R circulating water bath. The temperature was monitored within the cuvette with a 4-mm flexible thermistor attached to an Omega Model 747 digital thermometer.

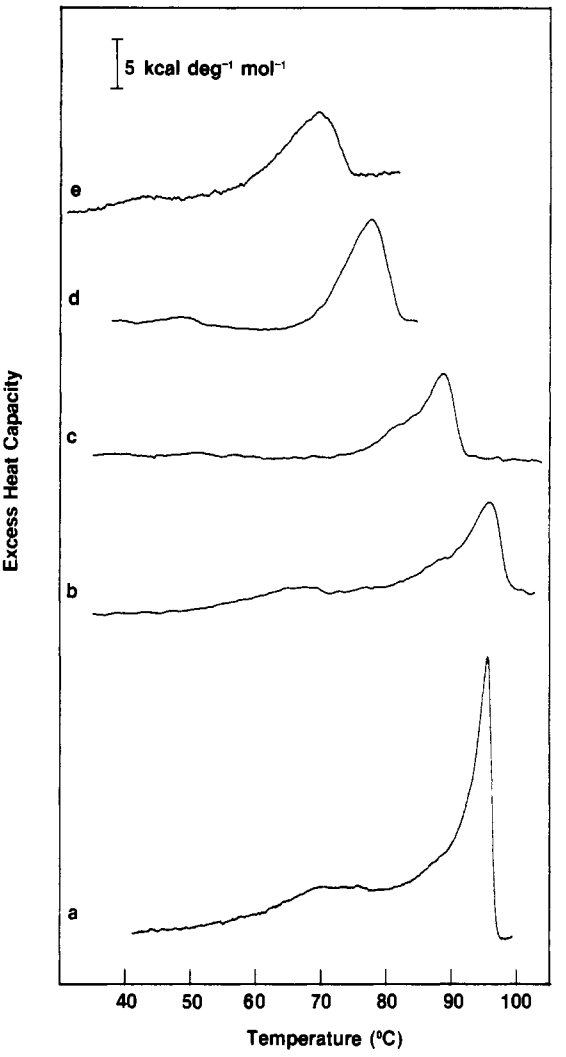

FIGURE 1: Differential scanning calorimetry of purple membrane (130 mM) at the indicated pH. The pH reported was measured at 25 °C; for glycine and glycylglycine, the approximate pH at T_m is indicated in parentheses; see text for details. All scans have had base lines subtracted except (a); see Materials and Methods for details. The scan rate was 85 deg/h. (a) pH 7.0, 190 mM phosphate; (b) pH 8.4 (6.6), 50 mM glycylglycine, 100 mM NaCl; (c) pH 9.6 (8.0), 50 mM glycine, 100 mM NaCl; (d) pH 9.8, 50 mM carbonate–bicarbonate, 100 mM NaCl; (e) pH 10.8, 50 mM carbonate–bicarbonate, 100 mM NaCl.

Circular Dichroism. The CD spectra were recorded with a Jasco J-500A spectropolarimeter interfaced to a DP-500N data processor. Spectra were recorded on 0.88 μM bacteriorhodopsin containing 190 mM phosphate, pH 8.5, at 20 nm/min on a sensitivity range of 0.5 mdeg/cm with a dynode voltage less than 400 V. Typically, 16 scans were averaged for both sample and reference, and the reported curves were obtained by digital subtraction. The temperature was adjusted by a Haake waterbath connected to a jacketed 2-mm cylindrical cell, and the cell temperatures were measured with a thermistor. The sample was allowed to equilibrate at each temperature prior to measurement.

RESULTS

Representative DSC profiles of purple membrane from pH 7.0 to pH 10.8 are shown in Figure 1. Calorimetry was performed on purple membranes in a total of 11 different buffers with and without NaCl up to a concentration of 400

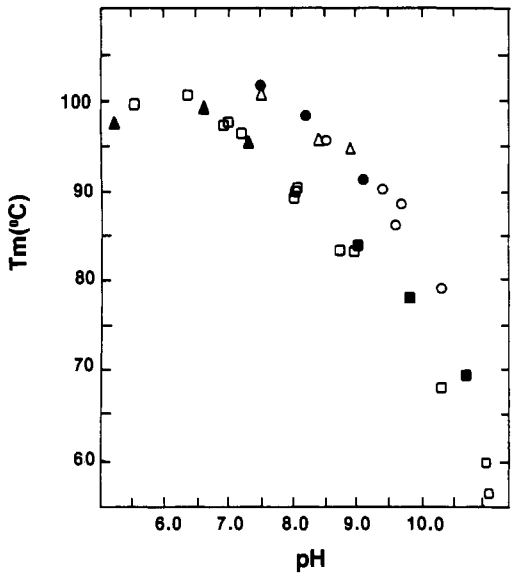

FIGURE 2: Denaturational midpoint temperature (T_m) as a function of pH. The pH reported was measured at 25 °C; see text for details. The symbols represent the following buffers: (square) 190 mM phosphate; (filled square) 50 mM carbonate–bicarbonate, 100 mM NaCl; (circle) 50 mM glycine, 100 mM NaCl; (filled circle) 50 mM tricine, 100 mM NaCl; (triangle) 50 mM glycylglycine, 100 mM NaCl; (filled triangle) 50 mM citrate, 100 mM NaCl.

mM. It was found that inclusion of 100 mM NaCl gave the most reproducible base lines for most of the buffers. Of the 11 buffers screened, 6 were chosen for quantitative analysis on the basis of reproducibility and base-line stability. There are several features of these scans to be noted. As indicated by the prominent denaturational transition, bacteriorhodopsin is most stable near pH 6.5 (Figure 2). The data points illustrated in Figure 2 tend to merge into a single curve, thereby reducing the apparent differences among the buffers in the measured T_m, when the known temperature dependence of the apparent pK_a of some of the buffers is taken into account (Good et al., 1966).[2] At pH values above 6.5, the denaturational transition temperature decreases with increasing pH. This transition is largely irreversible. Given time, however, the heated membrane will partially renature upon cooling, and the return of a purple hue and a denaturational transition of much lower enthalpy (approximately 10% of the original) on the second scan is seen. The denaturational transition is distinctly asymmetrical, and often a shoulder is discernible on the low-temperature side. Frequently, a positive heat capacity difference between the native and denatured states is apparent from the base line subtracted DSC profile. As discussed below, this is associated with a temperature-dependent denaturational enthalpy (Privalov, 1979).

Temperature-induced changes in bacteriorhodopsin spectra were also followed by UV, visible, fluorescence, and CD spectroscopies. In Figure 3 are typical spectra illustrating the changes due to temperature. Prior to denaturation, the visible absorbance maximum (λ_{max}) of bacteriorhodopsin shifts to shorter wavelengths. The shift of λ_{max} from about 560 nm to 460 nm appears to proceed through an isosbestic point and is reversible up to about 79 °C at pH 7.9 in glycylglycine (Figures 3A and 4A–C). At higher pH values, the spectral transition is largely, but not completely, reversible. Although much less prominent than the denaturational transition, a

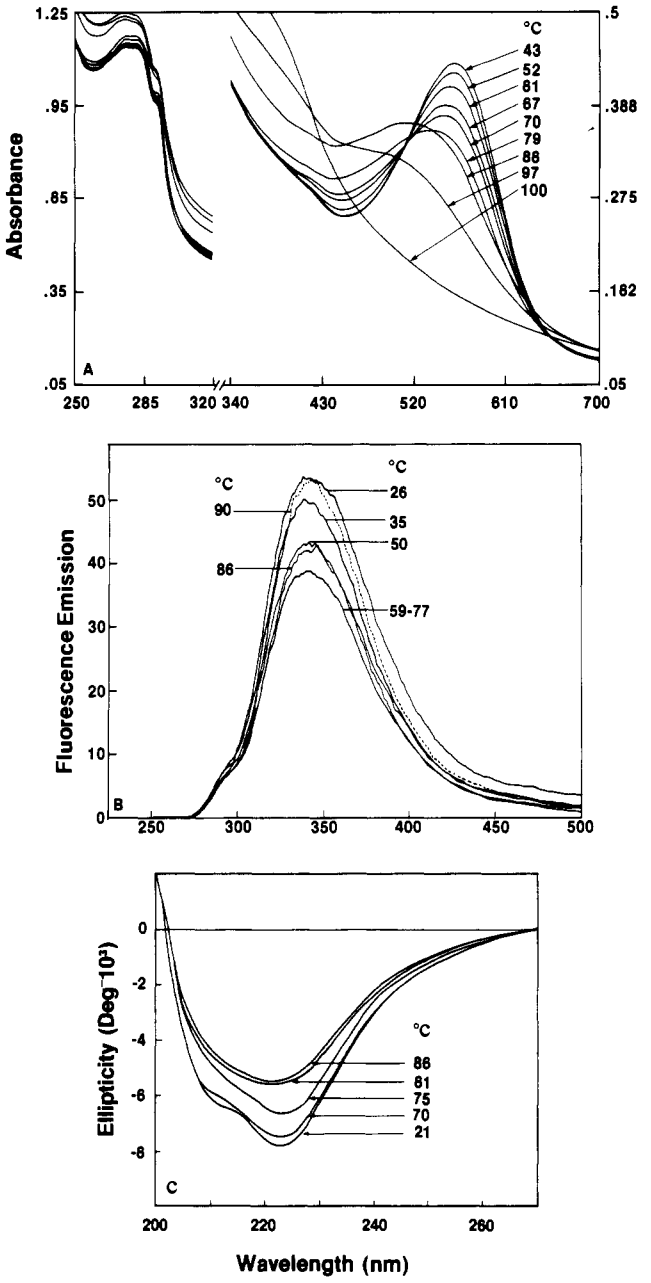

FIGURE 3: Temperature-dependent spectroscopy of the purple membrane. (A) Absorption spectroscopy in 50 mM glycylglycine and 100 mM NaCl, pH 7.9, at 25 °C (pH 6 at T_m). (B) Fluorescence spectroscopy in 50 mM glycine and 100 mM NaCl, pH 9.8 at 25 °C (pH 8 at T_m). (C) Circular dichroism in 190 mM phosphate, pH 8.5.

transition in this temperature region is observed by calorimetry as well (Figure 1). Denaturation of the protein is detected by a further shift in the visible absorbance to about 370 nm, concomitant with a change in absorbance at 280 nm and an increase in fluorescence emission at around 330 nm (Figure 3B). Above pH 10, only a decrease in emission is observed when the temperature is increased from 25 to 100 °C (data not shown). Far-UV CD is also sensitive to protein denaturation (Figure 3C). The negative ellipticity at 222 nm decreases by about 27%, indicating a reduction but not complete loss in α-helicity as the protein denatures (Figure 4C). The change in curve shape observed at high temperatures may be the result of an increase in light scattering, which is also observed in the absorption spectra.

Figure 5 shows a plot of the enthalpy of denaturation as a function of the midpoint temperature (T_m). A linear rela-

[2] Significant temperature-dependent changes in pH were found when tricine, glycine, and glycylglycine were used as buffers. Unless otherwise indicted, the pH values reported have been measured at 25 °C.

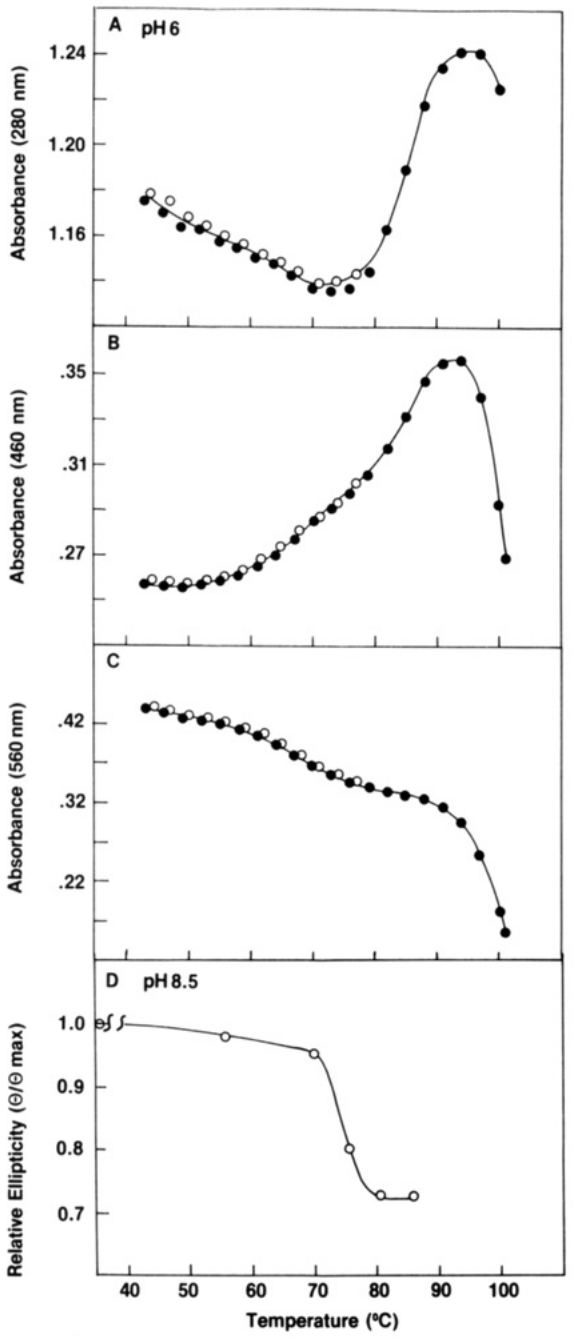

FIGURE 4: Temperature-dependent changes in the absorbance and circular dichroism of purple membrane at the indicated wavelength. (A–C) Absorption spectroscopy, derived from spectra shown in Figure 3A. Open symbols represent the initial heating experiment, after which the membrane was cooled to the temperature indicated by the first closed symbol and reheated. Closed symbols represent the repeated heating of the membrane. (C) Ellipticity at 222 nm relative to the maximum value observed at 21 °C; derived from spectra shown in Figure 3C.

tionship can be inferred that deviates at T_m values below 80 °C. The enthalpy was calculated from the area under the transition, extrapolating the base line through this temperature region. Modest alterations in the base line produced differences in the calculated enthalpy of less than 10% (<7 kcal/mol). At pH values of 8 and above, the purple membrane was adjusted immediately prior to the spectroscopic or calorimetric measurement to minimize pH-induced denaturation prior to the measurement. It was difficult to evaluate the extent of room temperature denaturation, although below pH 10 the membrane has been shown to be stable at room temperature (Muccio & Cassim, 1979). On the other hand, above pH 10

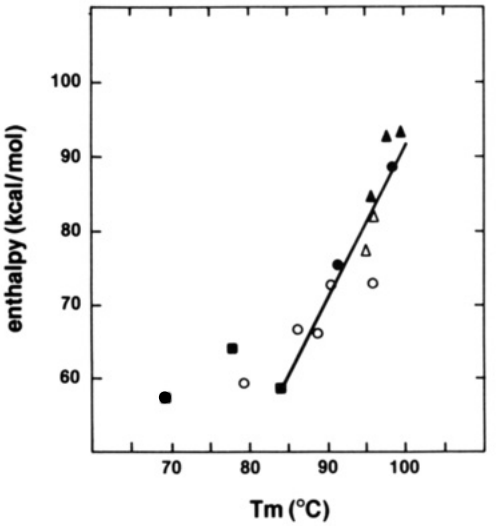

FIGURE 5: Denaturational enthalpy as a function of midpoint temperature (T_m). The symbol designations are the same as in Figure 2. Only DSC curves that had a good postdenaturational base line were used to calculate enthalpies for this plot. The line represents the least-squares fit of all points above 80 °C.

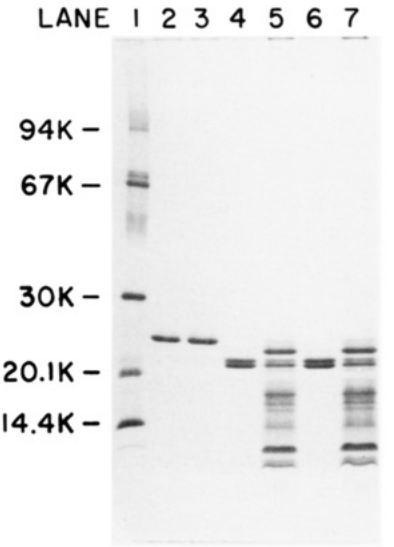

FIGURE 6: Proteolysis of native and denatured purple membrane. Purple membrane was incubated at 37 °C for 20 h with papain at a bacteriorhodopsin:papain weight ratio of 2.2:1. Samples were electrophoresed on a SDS–12–20% linear gradient polyacrylamide gel. (Lane 1) Protein standards; molecular masses (daltons) are indicated. (Lane 2) Purple membrane with no heat treatment prior to SDS solubilization for electrophoresis. (Lane 3) Purple membrane was heated at 100 °C for 3 min prior to SDS solubilization. (Lane 4) Purple membrane was treated with papain before SDS solubilization. (Lane 5) Purple membrane was heated at 100 °C for 3 min followed by treatment with papain prior to SDS solubilization. Lanes 6 and 7 are identical with lanes 4 and 5, respectively.

the spectral changes previously observed were not completely reversible, and the denaturational enthalpy at pH 10 decreased by about 25% when the membrane was allowed to stand at 4 °C for 18 h. Consequently, the apparent temperature-dependent enthalpy changes may, in part, be reflecting the room temperature instability of the purple membrane at high pH. The lack of linearity below 80 °C may also be attributed to this high-pH instability.

It was of interest to determine if denatured bacteriorhodopsin would exhibit an enhanced susceptibility to proteolysis over the native protein, as is often observed between native and unfolded soluble proteins. Proteolysis with papain was followed by SDS gel electrophoresis of the product, and

the results are shown in Figure 6. Papain hydrolyzes the peptide bonds of Arg (1.2), Lys (0.87), Glu (0.24), His (0.11), Leu (0.021), and Gly (0.014) in order of decreasing susceptibility (specific activities for the benzoyl or carbobenzoxy amides of the respective amino acids are given in parentheses; Kimmel & Smith, 1957). Prolonged reaction with papain yields additional cleavage sites (Hill, 1965). Papain treatment of native purple membrane produces two cleavage products (lane 4). The higher molecular weight product has been observed by others (Govindjee et al., 1982) and probably results from cleavage at Arg-227 in the exposed carboxyl tail. The product of lower molecular weight is consistent with cleavage at both Arg-227 and Arg-7. This newly observed product may be a result of the longer incubation time and larger papain:bacteriorhodopsin ratio employed here. As can be seen by comparison of lanes 4 and 5, heating the purple membrane through the denaturational transition results in extensive proteolysis by papain that does not occur to the native protein. The smallest proteolytic fragment observed for denatured bacteriorhodopsin has a molecular mass of 10.7 kDa, and fragments occur, on the average, every 890 Da. This degree of proteolysis is not seen in the native apomembrane (where the retinal group has been removed by reaction with hydroxylamine; Gerber et al., 1977) or if the purple membrane is heated to only 70 °C, which is below the temperature of denaturation at neutral pH, and then proteolyzed (data not shown).

Discussion

It seems reasonable to assume that most membrane proteins will adopt a structure composed of one or more compact globular domains as do the majority of soluble proteins (Kauzmann, 1959; Tanford, 1968, 1970; Brandts, 1969; Privalov & Khechinashvili, 1974). The transmission of a local structural perturbation (e.g., ligand binding) throughout the protein requires a level of cooperativity most easily achieved by a compact globular structure. Intuitively, one expects that the forces holding a membrane protein together will be different, at least in magnitude, from those of a soluble protein. However, neither the relative nor absolute magnitude of the interactions contributing to membrane protein stability is known. Several investigators have logically proposed that, in the absence of the hydrophobic effect, which plays a major role in the stability of water-soluble macromolecules, polar interactions must play a dominant role in maintaining the tertiary structure of an integral membrane protein like bacteriorhodopsin (Burres & Dunker, 1980; Engelman, 1982; Honig & Hubbell, 1984). Protein structural stability has been studied by the thermodynamic analysis of reversible protein unfolding or denaturation. Calorimetry offers a direct means for providing the thermodynamic values associated with protein structure and stability and has been utilized to study a number of membrane systems (Jackson et al., 1973; Jackson & Sturtevant, 1978; Cramer et al., 1981; Brouillette et al., 1982; Farach & Martinez-Carrion, 1983; Rigell et al., 1985). Unfortunately, in most cases, these systems have been too complex or have not been studied in adequate detail to enable a quantitative analysis of the results.

There have been two previous reports utilizing differential scanning calorimetry to study the purple membrane at neutral pH (Jackson & Sturtevant, 1978; Tristram-Nagle et al., 1986). The heat capacity profiles shown here at pH 7 in phosphate buffer compare well with those described in the earlier reports, which were also in phosphate buffer. It is clear from the present studies that buffer composition influences the shape of the denaturational transition. It is likely that the unfolding enthalpy is also influenced by this factor. In fact, the sulfonic acid buffers were completely unsuitable for these studies due to the occurrence of a large exotherm midway through the denaturational endotherm. These results suggest a postdenaturational exothermic event (perhaps aggregation) to be a factor that is affected to a variable extent by different buffers.

Pretransition. Although little emphasis has been placed on the reversible pretransition, we have made several interesting observations concerning this transition that relate to the tertiary and quaternary structure of bacteriorhodopsin. In the studies reported here, essentially no changes in secondary structure were observed through 70 °C at pH 8.5, by monitoring of ellipticity at 222 nm (Figure 4C). However, the changes we observe in the visible and near-UV absorption (Figures 3A and 4A–C) and fluorescence (Figure 3B) spectra suggest the possibility of tertiary structural changes in this temperature range. The most significant feature is the temperature-dependent shift in the visible absorbance maximum from a species absorbing near 560 nm to one absorbing around 460 nm. This wavelength shift is reversible (Figure 4A–C) and appears to proceed through an isosbestic point (Figure 3A). As the pH is increased, this transition occurs at lower temperatures. Ottolenghi and colleagues (Druckmann et al., 1982; Sheves et al., 1986) also observed a spectral change similar to this by varying pH at ambient temperature. The acid–base equilibrium between the 560- and 460-nm absorbing species was detected by briefly exposing the purple membrane to high pH. By utilizing resonance Raman spectroscopy on bacteriorhodopsin and on bacterioopsin containing artificial retinal analogues, they concluded that direct titration of the protonated Schiff base was responsible for the spectral changes they had observed.

Several reported studies have shown that significant quaternary structural changes occur in this temperature region. The present DSC measurements indicate the calorimetric pretransition is highly cooperative with a computed participation of approximately 8–40 protein monomers, depending on the solution conditions. Jackson and Sturtevant (1978) suggested the cooperativity of this transition was due to a structural reordering of the crystal lattice in this temperature region, and this was substantiated by the observation of a reversible temperature-induced change in the X-ray diffraction pattern of the purple membrane (Hwang & Stoeckenius, 1979; Hiraki et al., 1981). CD measurements in the visible region (Hiraki et al., 1981) suggest that a decrease in the order of the hexagonal packing occurs above the reversible pretransition, even though some trimers may still persist. Analysis of the X-ray diffraction pattern indicated that some intertrimer interactions may remain, although it is clear from both techniques that the long-range order has disappeared at temperatures above the pretransition. Our DSC results are consistent with these observations.

Denaturation. Bacteriorhodopsin is most stable to thermal denaturation near pH 6.5. Above this pH and most likely below, if the trend in Figure 2 can be extrapolated below pH 5.2, a pH-dependent decrease in thermal stability is seen. This behavior is very similar to the observed pH-dependent thermal denaturation of soluble proteins (Privalov, 1979). It is apparent from spectral measurements that principally tertiary structure is being lost when the protein denatures. As bacteriorhodopsin unfolds, retinal loses the characteristic protein contacts responsible for the purple color at 560 nm, resulting in a shift in the maximum to 370 nm. The fluorescence spectra of purple membrane in this temperature region show a significant increase in the relative fluorescence of the tryptophan

residues (Figure 3B). Nearly all the tyrosines and tryptophans are ordinarily quenched in the native state of bacteriorhodopsin through energy transfer to the retinal moiety. The observed dequenching is most simply interpreted as a loss of close contact between these residues and retinal as the protein unfolds, reflecting tertiary structural changes. From far-UV CD, comparatively smaller changes in the secondary structure occur as a result of thermal denaturation (Figure 3C). The observed decrease in negative ellipticity at 222 nm is consistent with some loss of α-helicity.

One would expect that, for a system at equilibrium, the pH denaturation at a fixed temperature should yield the same denatured state as the thermal denaturation at a fixed pH (Privalov, 1979). The pH denaturation of bacteriorhodopsin at a fixed temperature was shown by Muccio and Cassim (1979) to involve large changes in tertiary structure with only about a 20% reduction in ellipticity at 222 and 210 nm, which is very close to what has been observed here. Using the calorimetric data, specifically the plot of ΔH versus T_m from Figure 5, it is possible to draw similar conclusions regarding the residual structure of the denatured protein. Privalov (1979) has noted that for several simple globular proteins plots of the specific enthalpy of unfolding versus temperature intersected at about 110 °C, where ΔH is equal to 13 cal g^{-1}. The same was seen for the specific entropy, which was equal to 0.032 cal K^{-1} g^{-1} at about 110 °C. For bacteriorhodopsin, these values are considerably smaller (3.7 cal g^{-1} and 0.010 cal K^{-1} g^{-1}, respectively, at 110 °C) and could reasonably reflect a partially unfolded state for the denatured protein in the membrane. The curvature in this plot at low T_m values may be due to an isothermal pH-induced denaturation as previously discussed. A more reasonable explanation that is suggested by the fluorescence spectra is a change in the structure of denatured bacteriorhodopsin at high pH.

What may be the most interesting observation of these studies is the temperature dependence of the denaturational enthalpy, which is quite unexpected for an integral membrane protein that is completely sequestered from the aqueous environment (Figure 5). This behavior is characteristic of water-soluble proteins, where there is little question that it originates from the exposure of buried hydrophobic groups to the aqueous environment during unfolding (Brandts, 1969; Tanford, 1970; Privalov, 1979; Baldwin, 1986). If this interpretation holds for bacteriorhodopsin, one may envision that denaturation of the protein is accompanied by a disruption of the membrane. This would allow water to enter the hydrophobic interior and may result in irreversible exposure of the membrane-soluble portions of the protein to water. Alternatively, as the protein begins to unfold, the membrane may expand enough to allow transverse movement of the protein through it. A variety of chain topologies would result, which, due to the high protein density of the membrane, are unable to refold into the native state as the temperature is lowered. New aqueous protein loops would be generated from these alternate topologies, which would then be accessible to proteolysis. [In a different series of experiments, motion of transmembrane segments perpendicular to the membrane plane has been suggested as an explanation for the exposure of new cleavage sites to proteinase K digestion of bacteriorhodopsin (Dumont et al., 1985)]. Although both possibilities are consistent with the increased susceptibility to proteolysis observed (Figure 6), it is not possible to distinguish between them from the present studies.

For simple globular water-soluble proteins, the slope of the plot of enthalpy versus temperature (the denaturational heat capacity) is directly related to the fraction of hydrophobic residues the protein possesses (Privalov & Khechinashvili, 1974). The more hydrophobic residues exposed to water during unfolding, the greater is the denaturational heat capacity for the protein. For the most hydrophobic soluble protein that was studied (myoglobin), a slope of 0.155 cal K^{-1} g^{-1} was obtained. This value is more than 3 times the value we observe for bacteriorhodopsin, 0.046 cal K^{-1} g^{-1} (Figure 5). A value lower than anticipated for bacteriorhodopsin may indicate that the hydrophobic groups are not completely exposed to the aqueous environment during denaturation. This may be a consequence of the limited extent of unfolding (based on the far-UV CD) of bacteriorhodopsin as it denatures. As an alternative to the hydrophobic effect, we cannot rule out the possibility that the temperature-dependent enthalpy differences may, in part, be due to systematic differences in the extent of unfolding at different pH values.[3]

For an equilibrium, two-state process, the van't Hoff enthalpy is determined from the equilibrium constant, which, in this case, can be obtained directly from the calorimetric data (Jackson & Brandts, 1970; Sturtevant, 1974). The van't Hoff enthalpy can strictly be determined only for an equilibrium process, and for all practical purposes bacteriorhodopsin denaturation is not. The application of equilibrium thermodynamics to apparently irreversible processes has been discussed previously (Tanford, 1968; Privalov, 1982; Manly et al., 1985; Freire, 1987). Under certain conditions, we have observed that a repeat DSC scan does produce a small denaturational transition (up to 10% regeneration), and after being allowed to sit overnight, the yellow suspension of denatured membrane will partially recover its purple color, indicating that refolding is possible. The fact that Khorana and colleagues (Huang et al., 1981; London & Khorana, 1982) have successfully refolded denatured bacteriorhodopsin in the presence of detergents and free retinal suggests there is something inherent in the structural organization of the membrane, not necessarily the protein, which inhibits refolding after denaturation.

If both the van't Hoff and calorimetric enthalpies are known, the cooperativity of the process can be calculated from the ratio $\Delta H_{vH}/\Delta H_{cal}$. For a reversible two-state process, such as the denaturation of many soluble globular proteins (Privalov, 1979), this ratio will be very close to 1. A calculated value of less than 1 indicates the reaction is not two state, but proceeds through one or more intermediate states. A ratio greater than 1 is an indication of the size of the intermolecular cooperative unit. The average value of the ratio $\Delta H_{vH}/\Delta H_{cal}$ was determined to be 1.9 for the denaturational transition, from the data collected between pH 6 and pH 11; the individual values ranged nonsystematically from 1.3 to 2.7. [A value of nearly 2 was reported by Jackson and Sturtevant (1978)]. Due to the observed shoulder on the calorimetric

[3] A reviewer has duly noted that there are alternative driving forces that could be responsible for, or contribute to, the observed denaturational heat capacity change; for example, the exposure of buried polar or charged groups to water may result in a negative heat capacity change. This coupled with the positive heat capacity change associated with exposing hydrophobic groups would result in a lower than expected positive heat capacity as observed here. Although it is difficult to predict the heat capacity change, it is possible to calculate what may be the maxiumum contribution of exposing the putatively buried charged groups of bacteriorhodopsin to water from heat capacity values found in Sturtevant (1977) for the creation of a positive and negative pair of charges in aqueous solution. However, this is not enough to lower the heat capacity change to the value derived here for bacteriorhodopsin unfolding. In fact, comparison of bacteriorhodopsin with a soluble protein of comparable hydrophobicity would show a greater disparity between the expected and observed denaturational heat capacity.

transition, which may indicate the presence of another transition, the calculated values of $\Delta H_{vH}/\Delta H_{cal}$ may be underestimated. In addition to the shoulder, inspection of the denaturational transition reveals a distinct skewing of this peak. This is characteristic of the denaturation of oligomers, which is accompanied by their dissociation (Manly et al., 1985). Consistent with this interpretation is the DSC profile of monomeric bacteriorhodopsin in DMPC vesicles (prepared by detergent dialysis, at a lipid to protein ratio of 125:1). The denaturational transition of these preparations becomes broader, becomes more symmetrical, and lowers by about 15 °C (Brouillette, unpublished observation). The skewing of the denaturational transition in purple membrane could also be due to a postdenaturational exothermic process, although changes in the scan rate from 15 to 90 deg/h have no apparent affect on the asymmetry of the peak, as they might if an overlapping exotherm was present. Several lines of evidence suggest that at least a dimer if not the trimer of bacteriorhodopsin denatures as a cooperative unit in the purple membrane. Besides the calculated ratio of $\Delta H_{vH}/\Delta H_{cal}$ obtained from calorimetry for the denaturational transition, the temperature-dependent visible CD and X-ray diffraction studies of Hiraki et al. (1981) indicated that at temperatures prior to denaturation, but above the pretransition, trimers of bacteriorhodopsin were present. In light of the crystal structure of purple membrane (Henderson & Unwin, 1975), these results suggest an important role for the bacteriorhodopsin trimer in the structural stability of the purple membrane.

A topic not discussed so far is the role of the membrane lipids in the structural transitions of the purple membrane reported here. There are approximately 10 lipid molecules per protein molecule in the purple membrane, and by ^{31}P NMR, the phospholipids have been shown to be in a bilayer arrangement from 5 to 60 °C (Ekiel et al., 1981). Tristram-Nagle et al. (1986) detected a small transition near 25 °C by DSC that they interpreted as the melting of less than 25 degrees of freedom per bacteriorhodopsin molecule plus its associated lipids. In this temperature region ^{31}P NMR spectra showed a gradual line narrowing, and then, further line narrowing was observed above 67 °C (Haran et al., 1980). The line narrowing seen at higher temperatures may well correspond to the changes that occur in the crystal lattice associated with the reversible pretransition. No studies have explicitly addressed what happens to the purple membrane lipids when bacteriorhodopsin denatures. It seems reasonable to assume, however, that the lipids participate in the denaturational transition. Certainly, if gross disruption of the membrane occurs concomitantly with denaturation, this must involve the lipids. However, the extent to which protein–lipid interactions contribute to the unfolding enthalpy of bacteriorhodopsin is unknown.

Summary. A scenario of protein unfolding can be constructed for bacteriorhodopsin from this study and key observations previously made by others. Prior to denaturation, bacteriorhodopsin undergoes at least one temperature-dependent reversible structural transition within the purple membrane that leads to a diminution in intermolecular cooperativity; i.e., long-range interactions between the trimers are lost. Changes in the tertiary structure of the protein also occur and may be principally localized near the retinal moiety. Preliminary data on detergent-solubilized monomeric bacteriorhodopsin suggests a similar conformational change occurs in the protein of this preparation prior to denaturation (Brouillette, 1987). In the purple membrane, therefore, the reversible pretransition most likely represents the transmission throughout the membrane of a protein conformational change. In view of the macromolecular organization of the purple membrane, the intermolecular cooperativity of this predenaturational transition is not surprising. Following the reversible pretransition, bacteriorhodopsin denaturation is accompanied by a further loss of quaternary and tertiary structure. Apparently smaller changes in secondary structure occur relative to these changes, as well as in comparison to the loss in secondary structure that is normally associated with the unfolding of water-soluble proteins. The denaturational enthalpy at 110 °C is somewhat lower than that of soluble proteins, possibly reflecting this incomplete unfolding. As bacteriorhodopsin unfolds, the trimers probably dissociate, and in the process bacteriorhodopsin is either extruded from the membrane or reorients, exposing hydrophobic domains to water. Although the difference in heat capacity between native and denatured bacteriorhodopsin is significantly less than the values obtained for water-soluble proteins, these results lead to the intriguing possibility that the hydrophobic effect contributes to the stabilization free energy of this membrane protein, as it does for all soluble proteins.

ACKNOWLEDGMENTS

We sincerely thank Drs. John Brandts, James Matthew, Ernesto Freire, Barbara Lewis, and Joyce Jentoft for the helpful discussions and advice given over the course of this work and Ruth McMichens for expert technical assistance.

REFERENCES

Agard, D. A., & Stroud, R. M. (1982) *Biophys. J. 37*, 589.
Baldwin, R. L. (1986) *Proc. Natl. Acad. Sci. U.S.A. 83*, 8069.
Becher, B., & Cassim, J. Y. (1975) *Prep. Biochem. 5*, 161.
Becher, B., & Cassim, J. Y. (1976) *Biophys. J. 16*, 1183.
Brandts, J. F. (1969) in *Structure and Stability of Biological Macromolecules* (Timasheff, S. N., & Fasman, G. D., Eds.) p 213, Dekker, New York.
Brouillette, C. G. (1987) *J. Cell. Biochem., Suppl. 11c*, 233.
Brouillette, C. G., Compans, R. W., Brandts, J. F., & Segrest, J. P. (1982) *J. Biol. Chem. 257*, 12.
Brouillette, C. G., Muccio, D. D., & Barton, J. S. (1986) *Biophys. J. 49*, 474a.
Burres, N., & Dunker, A. K. (1980) *J. Theor. Biol. 87*, 723.
Cramer, W. A., Whitmarsh, J., & Low, P. S. (1981) *Biochemistry 20*, 157.
Dencher, N. A., Kohl, K.-D., & Heyn, M. P. (1983) *Biochemistry 22*, 1323.
Downer, N. W., Bruchman, T. J., & Hazzard, J. H. (1986) *J. Biol. Chem. 261*, 3640.
Druckmann, S., Ottolenghi, M., Pande, A., Pande, J., & Callender, R. H. (1982) *Biochemistry 21*, 4953.
Dumont, M. E., Trewhella, J., Engelman, D. M., & Richards, F. M. (1985) *J. Membr. Biol. 88*, 233.
Earnest, T., & Rothschild, K. (1986) *Biophys. J. 49*, 294a.
Ekiel, I., Marsh, D., Smallbone, B., Kates, M., & Smith, I. (1981) *Biochem. Biophys. Res. Commun. 100*, 105.
Engelman, D. M. (1982) *Biophys. J. 37*, 187.
Engelman, D. M., Henderson, R., McLachlan, A. D., & Wallace, B. A. (1980) *Proc. Natl. Acad. Sci. U.S.A. 77*, 2023.
Farach, M. C., & Martinez-Carrior, M. (1983) *J. Biol. Chem. 258*, 4166.
Freire, E. (1987) *Biophys. J. 51*, 381a.
Gerber, G., Gray, C., Wildenauer, D., & Khorana, G. (1977) *Proc. Natl. Acad. Sci. U.S.A. 74*, 5426.
Good, N., Winget, G., Winter, W., Connolly, T., Izawa, S., & Singh, R. (1966) *Biochemistry 5*, 467.

Govindjee, R., Ohno, K., & Ebrey, T. (1982) *Biophys. J. 38*, 85.
Haran, N., Hwang, S. B., & Hall, F. W. (1980) *Fed. Proc., Fed. Am. Soc. Exp. Biol. 39*, 840A.
Henderson, R. (1977) *Annu. Rev. Biophys. Bioeng. 6*, 87.
Henderson, R., & Unwin, N. (1975) *Nature (London) 257*, 28.
Hill, R. (1965) *Adv. Protein Chem. 20*, 37.
Hiraki, K., Hamanaka, T., Mitsui, T., & Kito, Y. (1981) *Biochim. Biophys. Acta 647*, 18.
Honig, B., & Hubbell, W. (1984) *Proc. Natl. Acad. Sci. U.S.A. 81*, 5412.
Huang, K.-S., Bayley, H., Liao, M.-J., London, E., & Khorana, H. G. (1981) *J. Biol. Chem. 256*, 3802.
Hwang, S.-B., & Stoeckenius, W. (1979) *Biophys. J. 25*, 207a.
Jackson, M. B., & Sturtevant, J. M. (1978) *Biochemistry 17*, 911.
Jackson, W. M., & Brandts, J. F. (1970) *Biochemistry 9*, 2294.
Jackson, W. M., Kostyla, J., Nordin, J. H., & Brandts, J. F. (1973) *Biochemistry 12*, 3602.
Jap, B. K., Maestre, M. J., Hayward, S. B., & Glaeser, R. M. (1983) *Biophys. J. 43*, 81.
Kauzmann, W. (1959) *Adv. Protein Chem. 14*, 1.
Khorana, H. G., Gerber, G. E. Herlihy, W. C., Gray, C. P., Anderegg, R. J., Nihei, K., & Biemann, K. (1979) *Proc. Natl. Acad. Sci. U.S.A. 76*, 5046.
Kimmel, J., & Smith, E. (1957) *Adv. Enzymol. Relat. Subj. Biochem. 19*, 267.
Lewis, B. A., Harbison, G. S., Herzfeld, J., & Griffin, R. G. (1985) *Biochemistry 24*, 4671.
London, E., & Khorana, H. G. (1982) *J. Biol. Chem. 257*, 7003.
Manly, S. P., Matthews, K. S., & Sturtevant, J. M. (1985) *Biochemistry 24*, 3842.
Mao, D., & Wallace, B. A. (1984) *Biochemistry 23*, 2667.
Marque, J., Eisenstein, L., Gratton, E., Sturtevant, J. M., & Hardy, C. J. (1984) *Biophys. J. 46*, 567.
Muccio, D. D., & Cassim, J. Y. (1979) *J. Mol. Biol. 135*, 595.
Nabedryk, E., Bardin, A. M., & Breton, J. (1985) *Biophys. J. 48*, 873.
Oesterhelt, D., & Stoeckenius, W. (1971) *Nature (London), New Biol. 233*, 149.
Ovchinnikov, Y., Abdulaev, N., Fergina, M., Kiselev, A., & Lobanov, N. (1979) *FEBS Lett. 100*, 219.
Privalov, P. L. (1979) *Adv. Protein Chem. 33*, 167.
Privalov, P. L. (1982) *Adv. Protein Chem. 35*, 1.
Privalov, P. L., & Khechinashvili, N. N. (1974) *J. Mol. Biol. 86*, 665.
Rigell, C. W., de Saussure, C., & Freire, E. (1985) *Biochemistry 24*, 5638.
Sheves, M., Albeck, A., Friedman, N., & Ottolenghi, M. (1986) *Proc. Natl. Acad. Sci. U.S.A. 83*, 3262.
Sturtevant, J. M. (1974) *Annu. Rev. Biophys. Bioeng. 3*, 35.
Sturtevant, J. M. (1977) *Proc. Natl. Acad. Sci. U.S.A. 74*, 2236.
Tanford, C. (1968) *Adv. Protein Chem. 23*, 121.
Tanford, C. (1970) *Adv. Protein Chem. 24*, 1.
Tristram-Nagle, S., Yang, C.-P., & Nagle, J. F. (1986) *Biochim. Biophys. Acta 854*, 58.
Wallace, B. A., & Henderson, R. (1982) *Biophys. J. 39*, 233.

Thermodynamic Parameters of Cytochrome c_3–Ferredoxin Complex Formation

Françoise Guerlesquin,*,‡ Jean-Claude Sari,§ and Mireille Bruschi‡

Laboratoire de Chimie Bactérienne, CNRS, 13277 Marseille Cedex 09, France, and Laboratoire de Physique et de Biophysique, Faculté de Pharmacie, 13385 Marseille Cedex 04, France

Received February 23, 1987; Revised Manuscript Received July 2, 1987

ABSTRACT: The complex formation between cytochrome c_3 and ferredoxin I from *Desulfovibrio desulfuricans* Norway was studied by microcalorimetric and pH-stat titration measurements. The stoichiometry of the complex was found to be one molecule of cytochrome c_3 per monomer of ferredoxin I. The association constant determined at $T = 283$ K in tris(hydroxymethyl)aminomethane hydrochloride (Tris-HCl) buffer, 10^{-2} M and pH 7.7, was $K_A = 1.3 \times 10^6$ M^{-1}. Though the enthalpy ($\Delta H = 19 \pm 1$ kJ·mol^{-1}) and the entropy ($\Delta S = 183$ J·K^{-1}·mol^{-1}) were positive and consistent with a hydrophobic process involved in the interaction, the analysis of ionic strength dependence exhibited an important electrostatic effect on the association. The use of both Tris-HCl and phosphate buffers during microcalorimetric experiments showed proton release at pH 6.6. The pH-stat study of proton release indicated that one of the charged groups involved in the interacting site underwent a pK shift from 7.35 to 6.05.

Oxidation–reduction reactions between two metalloproteins necessitate the formation of an intermediate complex in which the redox centers of the two proteins are optimally oriented to achieve physiological electron transfer (Poulos & Kraut, 1980). Various protein–protein interaction studies have been recently reported on the basis of crystallographic information, NMR data, chemical modifications, or covalent cross-linking experiments. Cytochrome c is one of the most investigated electron carrier proteins. Complex formation between cytochrome c and both physiological and nonphysiological partners have been studied: cytochrome c–cytochrome c peroxidase (Poulos & Kraut, 1980; Waldmeyer & Bosshard, 1985), cytochrome c–cytochrome b_5 (Salemme, 1976; Eley & Moore, 1983), and cytochrome c–flavodoxin (Simondsen et al., 1982; Hazzard & Tollin, 1985; Dickerson et al., 1985). In these models the prosthetic groups are nearly coplanar, separated by a distance of about 10 Å, and the specificity of the interaction is provided by the ϵ-amino groups on cytochrome c and carboxyl groups on its partner. Moreover, a hydrophobic

‡ Laboratoire de Chimie Bactérienne.
§ Laboratoire de Physique et de Biophysique.

0006-2960/87/0426-7438$01.50/0